清华大学博士后科学论文集

闫　超

清华大学出

清华大学博士后科学论文集

阎　超等

清华大学出版社

内 容 简 介

清华大学云集众多博士后青年学者，在流动站期间发表了许多很有价值的论文。本论文集选编了31篇论文。内容涉及土建、机械、精密仪器、电机电子、力学和经济管理等学科以及跨学科的问题。论文集的论文论述的学科前沿问题和科学技术深层次的问题，对科学研究和国民经济发展会提供有益的帮助。

本论文集可供有关学科的教师、研究生和科研人员、工程技术人员参考。

(京)新登字158号

清华大学博士后科学论文集

阎 超 等

☆

清华大学出版社出版

北京 清华园

清华大学印刷厂印刷

新华书店总店科技发行所发行

☆

开本：787×1092 1/16 印张：14.25 字数：338千字

1992年6月第1版 1992年6月第1次印刷

印数：0001—1600

ISBN 7-302-00999-6/Z·51

定价：10.80元

前　言

博士后流动站是我国根据社会主义建设需要而建立的一项新的制度。目的是为优秀留学博士回国工作创造条件、加强国内人材和学术交流并造就一批科技新秀。我校自1985年底成立博士后流动站以来，至今已建立11个博士后流动站，覆盖了45个博士点，共招收了88名获博士学位的优秀青年。几年来的实践表明，他们已成为清华大学科研工作中的生力军。据对期满离站的30位博士后成果的统计表明，他们大都在国家重大项目中担负重任，每位博士后在站期间平均承担2项以上科研任务，发表学术论文6篇，大部分成果达到了国际或国内先进水平。在作出这些贡献的同时也促进了不少优秀人材脱颖而出。“清华大学博士后科学论文集”本身就是博士后流动站取得很大成就的一个明证，我相信，“清华大学博士后科学论文集”的出版必将进一步推动博士后间的学术交流，促进博士后的科研成果更好更快地为我国四化建设服务，祝愿博士后流动站更加兴旺发达。

梁尤能

3.19

目　录

SHEAR TRANSFER MODEL FOR CRACKED REINFORCED CONCRETE

Baolu Li

Laboratory of Building Materials

Department of Civil Engineering, Tsinghua University

ABSTRACT

A method for calculating the ultimate shear strength and deformational behavior along cracks in reinforced concrete is proposed by combining shear transfer model for crack in plain concrete and bond-slip-strain model, taking into account of the bond deterioration due to separation and crushing of concrete around reinforcing bar. Results of a series of experiments show that such a consideration holds well for specimens with different reinforcement ratios, bar diameters and concrete compressive strengths.

1. INTRODUCTION

Shear transfer problem across cracks in reinforced concrete can arise inevitably because of shrinkage, tensile stress or some other unforeseen reasons. Such a situation may frequently occur in the design of precast concrete connection, corbels, brackets and beamcolumn connection. The deformational behavior and ultimate strength of reinforced concrete structure may be considerably affected by the occurrence of one or more cracks. On the other hand, RC shear Wall, RC containments and shell structures are usually subjected to sectional forces which may be caused by earthquake, inner pressure and other mechanical loads. Finite element method is frequently used for the analysis of these structures. However, the mechanical behavior can be predicted only when the behavior of their component element, i. e. RC element is known well.

Experimental studies on shear transfer were performed by many investigators, factors including the characteristics of shear plane, the characteristics of reinforcement, concrete compressive strength and direct stress acting parallel or transverse to the shear plane have been discussed [1,2]. In the present paper, the shear transfer model derived from so-called contact density function for plain concrete is extrapolated to the case of reinforced concrete where reinforcing bars intersects the crack plane in concrete.

2. SHEAR TRANSFER MODEL AND BOND-SLIP-STRAIN MODEL

2. 1 Shear Transfer Model for Plain Concrete

A unit area of concrete crack surface was modeled as a set of infinite potential contact planes with different directional angle θ, which is described by a probability density function $\cos(\theta)$. A simple formula for shear transfer behavior across cracks under monotonic loading was obtained by using rigid-plastic model to represent the relationship between contact stress and deformations in crack plane[3].

$$\tau = m \frac{\delta^2}{\delta^2 + \omega^2}$$
$$\sigma = m\left[\frac{\pi}{2} - \tan^{-1}\frac{\omega}{\delta} - \frac{\delta\omega}{\delta^2 + \omega^2}\right] \tag{1}$$
$$m = 3.826\ fc'^{1/3}(\text{MPa}).$$

where fc' is the compressive strength of cylindrical specimen, τ and σ are shear and compressive stress in MPa, δ and ω are shear displacement and crack opening in millimeter respectively.

2. 2 Bond-Slip-Strain Relationship for Reinforcing Bar in Concrete

Shima[4] etc. have experimentally derived a bond-slip-strain relation from pull-out tests, which gives precise prediction when deformed bar is pulled out of massive concrete body. The bond-slip-strain relation was formulated as,

$$\frac{\tau_b}{f'_c} = 0.73\frac{\ln^3(1 + 5 \cdot \zeta)}{1 + \varepsilon \cdot 10^5} \tag{2}$$

where $\zeta = \frac{S}{D} \cdot 1000$ (non-dimension)

τ_b : bond stress (MPa)

fc' : concrete cylindrical compressive strength (MPa)

s : slip between reinforcement and concrete (mm)

D : bar diameter used as reinforcement (mm)

ε : strain of reinforcement at the concerned position

At position x, which is the distance from the free end of specimen along the reinforcement, the following equations are valid,

$$\tau_b(x) = \tau_b(s(x), \varepsilon(x)) \qquad (\textit{from Eq. (2)}) \tag{3}$$

$$s(x) = s_0 + \int_0^x \varepsilon(x)dx \tag{4}$$

$$\sigma_s(x) = E \quad \varepsilon(x) \qquad (\sigma - \varepsilon \ \textit{relation of steel before yielding}) \tag{5}$$

$$\tau_b(x) = \frac{D}{4}\frac{d\sigma_s(x)}{dx} \quad (equilibrium\ equation) \tag{6}$$

where s_0 is slip at free end of reinforcement ($x=0$) and $\sigma_s(x)$ the tensile stress of reinforcement at point x. By solving these simultaneous equations(3,4,5,6), ε, τ_b and s can be calculated at any position of the reinforcement for a given stress σ_s.

3. SHEAR STRENGTH OF INITIALLY CRACKED REINFORCED CONCRETE

3.1 Aggregate Interlock and Dowel Action

Aggregate interlock and dowel action are two main mechanisms to resist shear stress along crack. However, shear transfer characteristics may hardly be represented as a simple algebraic summation of aggregate interlock and dowel effect because they are interdependent and not easy to separate. Their proportions may change with reinforcement ratio, stirrup content, covering thickness of reinforced bar, surface asperities of bar, bond effect between steel bar and concrete around, et al.

Irrespective of the difficulties to evaluate the contribution of aggregate interlock and dowel action separately, many researchers have recognized that dowel action plays a minor role compared to aggregate interlock[5], and may be ignored in most situations in reinforced concrete members.

3.2 Shear Strength of Cracked Reinforced Concrete

The relation between shear and compressive stresses along cracked concrete can be derived from Eq. (1),

$$\tau = \tau(\sigma)$$

$$or\ \sigma = \sigma(\tau)$$

$$= m\left[\frac{\pi}{2} - \tan^{-1}\left(\frac{m}{\tau} - 1\right)^{1/2} - \frac{(m/\tau - 1)^{1/2}}{m/\tau}\right] \tag{7}$$

where m is a function of concrete compressive strength only, shear strength can be calculated easily if confining stress σ is given.

Mattock etc. have carried out a series of experiments to study the shear strength of precracked concrete using push-off type specimen(Fig. 1).

Fig. 2(a) is the comparison between Mattock's experimental results and the calculated values using Eq. (7), the average ratio of tested strengths to calculated ones η is 0.93 and the co-

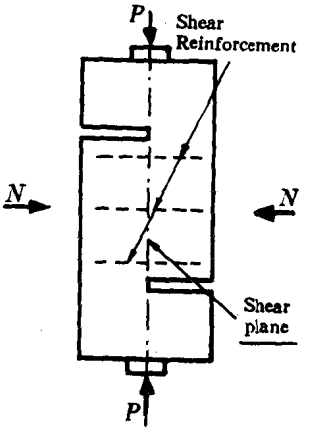

Fig. 1 Push-off Specimen

efficient of variation C. V. is 14%.

In RC structure, external compressive or tensile forces may also be applied in the direction normal to a crack plane. The reinforcement is usually in tension and concrete in compression. In Fig. 2(*b*), where positive sign of normal stress corresponds to compression and negative one to tension, the experimental results for both external compression and tension cases were predicted well by Eq. (7), with $\eta=0.98$ and C. V. $=7.47\%$.

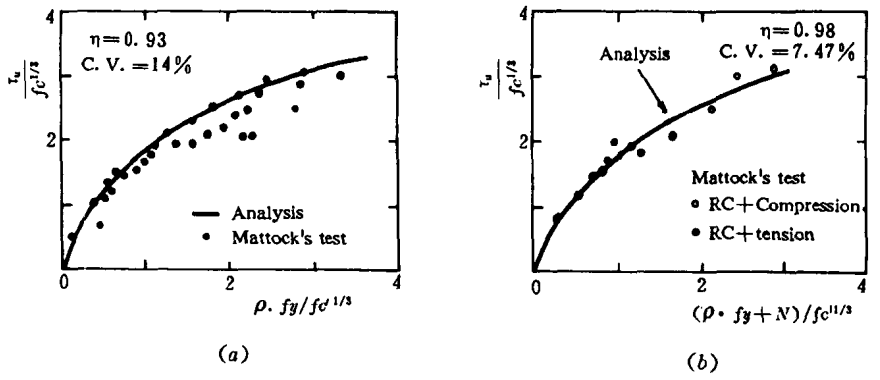

Fig. 2(a) Push-off Test (b) Push-off with External Force Acting on Shear Plane

Eq. (7) concerns only interlock effect of aggregate, consequently the effect of dowel action caused by the presence of reinforcement on ultimate shear strength of concrete crack plane can obviously be neglected compared with interlock shear resistance.

4. DEFORMATIONAL BEHAVIOR OF CRACKED REINFORCED CONCRETE

4.1 Experimental Outline

To study the deformational behavior of initially cracked reinforced concrete, reinforced concrete beams were used, test set-up and loading arrangement are shown in Fig. 3.

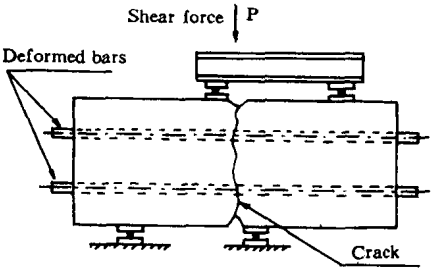

Fig. 3 Test Set-up of Reinforced Concrete

Specimens with different reinforcement ratio, 0.70% and 1.88%, were cast. Properties of all reinforced concrete test set up of specimens are shown in Table 1.

Aggregate having 15mm maximum size was supplied for all specimens. The deformed bar with screw-shaped texture was used as reinforcement. Various sections were to provide sufficient concrete covering thickness for the reinforce-

ment having different bar diameters. Relatively long specimens were provided to ensure that there was apparently no slip and no strain at the free end of the embedded bars. Crack was introduced by splitting load prior to testing.

Table 1 Properties of Reinforced Concrete Specimens

Specimens			Reinforcement					Concrete
No.	section mm x mm	L mm	ρ %	D	number	fy' MPa	E 10^5MPa	fc' MPa
RC-1	150x300	600	0.71	D19	1	389	1.92	41.3
RC-2	150x300	900	0.71	D10	4	429	2.05	32.8
RC-3	200x300	1500	1.88	D25	2	456	1.91	28.0

4.2 Combination of Shear Transfer and Bond-Slip Behavior

In prior sections, the contribution of dowel action to ultimate shear strength was discussed and generally its effect may be ignored if compared with aggregate interlock effect. It can be assumed that the role of reinforcement perpendicular to crack plane is to supply compression to concrete in the direction normal to the crack surface, the compressive stress in turn increase the shear capacity along crack, which is as "shear friction". Consequently the reinforcement has no directly significant influence on carrying shear stress.

By combining the so-called bond-strain-slip relation with shear transfer model for monotonic loading and assuming that the amount of pull-out of reinforcement from concrete body be the same with average crack width, τ-δ and ω-δ relations of any initially cracked reinforced concrete can be obtained. At crack plane,

$$s = s_0 + \int_0^{L'} \varepsilon(x)dx \tag{8}$$

$$L' = L/2 \tag{9}$$

$$\sigma_s = \rho\sigma_c \qquad (\textit{equilibrium equation between reinforcing bar and concrete}) \tag{10}$$

$$\sigma_c = \sigma_c(\omega,\delta) \qquad (\textit{from Eq. (1)}) \tag{11}$$

$$\tau_c = \tau_c(\omega,\delta) \qquad (\textit{from Eq. (1)}) \tag{12}$$

$$\omega = 2s \tag{13}$$

where L is the specimen length, L' is the embedded length of reinforcement, subscript c refers to concrete and ρ is the reinforcement ratio.

One example is shown in Fig. 4(a,b) by dashed lines, experimental result is also plotted in the same figure for comparison. As can be seen from these figures, predicted shear stiffness is relatively higher by the method explained above. The authors recognized that the test conditions between pull-out specimen used for deriving bond-slip-strain model and shear transfer specimen

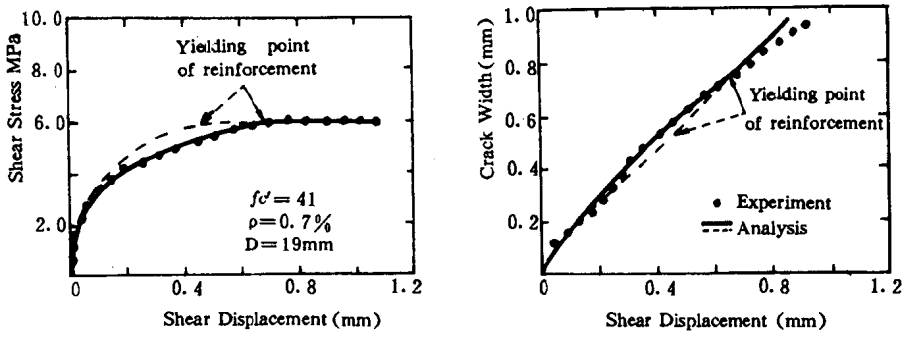

(a) (b)

Fig. 4 RC-1 (a) τ-δ Relation (b) ω-δ Relation

used in the present study are not exactly the same. The stress states of the reinforcement are different between the two tests. It carry pure tension only in pull-out test but carry tension, shear and perhaps bending in shear transfer test (Fig. 5). The concrete close to reinforcement at crack surface may be split or crushed seriously that no more bond stress can be carried. Taking this into account, more accurate shear stiffness was obtained as shown in the same figure illustrated by solid line (Fig. 4), by assuming that the bond stress τ_b near the crack ($x=L/2$) is zero in the shear transfer test. Eq. (9, 13) are rewritten and more are added in the modified model.

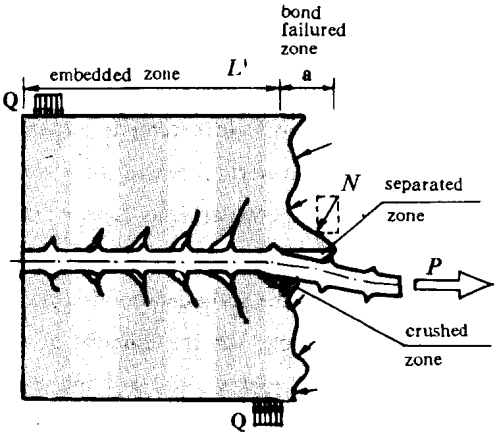

Fig. 5 Mechanism of Shear Transfer

$$L'=\frac{L}{2}-a \tag{9'}$$

$$\omega=2[s+a\varepsilon(x=L/2)] \tag{13'}$$

$$a=\alpha D \tag{14}$$

$$\alpha=2 \tag{15}$$

"a" refers to the range in $L/2$ near crack where no bond stress exists between reinforcement and concrete, which is due to the bond deterioration caused by crushing of concrete and the testing conditions. Herein "a" is taken to be proportional to the diameter of the reinforcement D. ε ($x=L/2$) is the strain of reinforcement at crack, and α is bond deterioration coefficient determined empirically.

Such an assumption can also give reasonable prediction to the deformational path as the solid

line in Fig. 4(*b*).

For other two experiments, RC-2 had same reinforcement ratio but different bar diameter, RC-3 had different reinforcement ratio and different bar diameter, their shear deformational behaviors were simulated well as shown in Fig. 6 and Fig. 7 respectively.

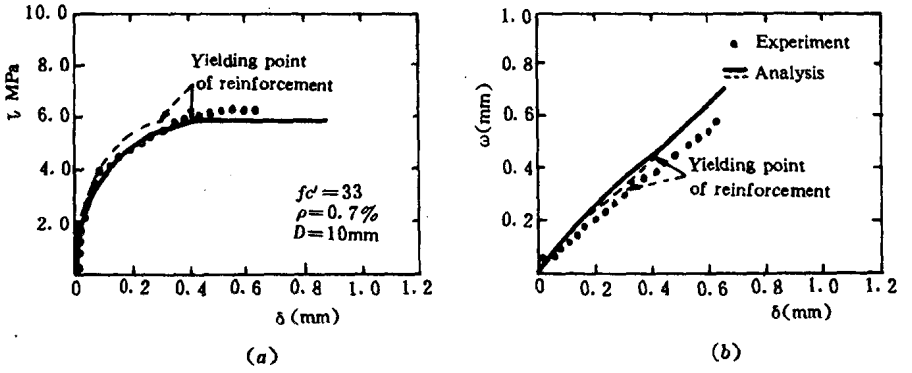

Fig. 6 RC-2 (*a*) τ-δ Relation (*b*) ω -δ Relation

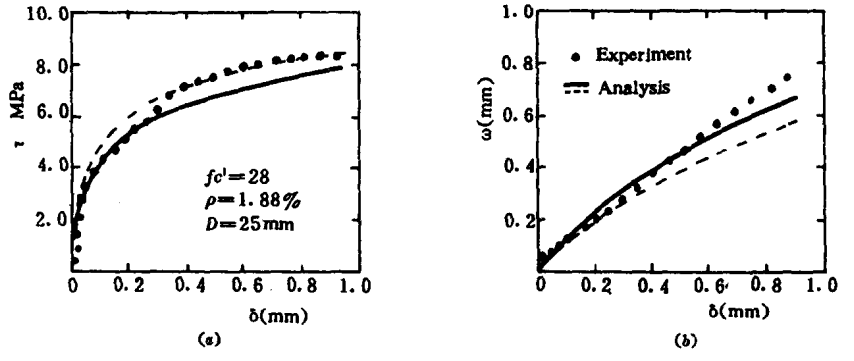

Fig. 7 RC-3 (*a*) τ-δ Relation (*b*) ω -δ Relation

So far, the mechanism of dowel action can be concluded, namely, concrete away from the crack surface can carry bond stress with reinforcement, while the area close to crack surface and around reinforcement will be partly crushed due to bearing effect of the reinforcing bar. This possibly results in reduction of dowel action contribution to shear transfer along cracks.

5. CONCLUSIONS

Shear strength simulation of cracked concrete derived for plain concrete under monotonic loading path can easily be extended to be used in the case of initially cracked reinforced concrete plane with reinforcement embedded in the direction normal to the crack plane, including the case where external compressive or tensile force acts transversely to the crack plane before and during

shear loading. The ultimate shear transfer stress will be achieved atfer yielding of reinforcement.

Deformational behavior of cracked reinforced concrete plane can be simulated appropriately by combining the bond-slip-strain model with the shear transfer model, taking account of the bond deterioration near crack surface in shear transfer test. Such a consideration holds well for specimens with different reinforcement ratios, bar diameters and concrete compressive strengths. However, further work is necessary for collecting additional data to prove the validity of the empirical hypothesis which ignored the bond effect between concrete and reinforcement near crack surface in the range $a=\alpha D$, and more modification may be needed.

REFERENCES

[1] Mattock A. H. and Howkins N. M. , "Shear Transfer in Reinforced Concrete Recent Research," PCI Journal, Mar. -Apr. 1972.

[2] Hofbeck J. A. , Ibrahin I. O. and Mattock A. H. , "Shear Transfer in Reinforced Concrete," ACI Journal, Vol. 66, No. 2, Feb. 1969.

[3] Li B. L. and Maekawa K. , "Contact Density Model for Cracks in Concrete," IABSE Colloquium, Delft 1987.

[4] Shima H. , Chou L. L. and Okamura H. , "Bond-Slip-Strain Relationship of Deformed Bars Embedded in Massive Concrete," Concrete Library of JSCE, No. 10, Dec. 1987.

[5] Walraven J. C. and Reinhardt H. W. , "Theory and Experiments on The Mechanical Behavior of Crack in Plain and Reinforced Concrete Subjected to Shear Loading," HERON, Vol. 26, No. 1A,1981.

脆性材料压-拉强度比的估计

姚卫星　俞新陆　颜永年

（清华大学机械工程系）

摘　要

本文按最大拉应力破坏准则分析了脆性材料中含有两类不同缺陷（空洞形缺陷和片状缺陷）时的压-拉强度比。对于空洞形缺陷压-拉强度比在2～8倍之间，对于片状缺陷压-拉强度比可以是大于1.9的任意值。这一结论很好地解释了某些高性能陶瓷压-拉强度比的实验结果。

一、引　言

脆性材料（如玻璃、陶瓷等）在直至破坏的整个变形过程中无塑性变形出现。这类材料的压缩强度要比拉伸强度高，有的甚至高出几十倍（如：氧化铝陶瓷压-拉强度比为12倍[1]，氧化锆陶瓷压-拉强度比为7.1倍[2]），本文作者做了氮化硅陶瓷SN-220的拉伸和压缩强度试验，得到SN-220的压-拉强度比约为20倍[3]。

脆性材料的强度取决于它们内部的缺陷。一般地可将缺陷划分为两大类：空洞形缺陷和片状缺陷。空洞形缺陷可用椭球来表征，片状缺陷可用便士形裂纹来表征。文献[4]利用椭圆形缺陷模型按最大拉应力准则得出压-拉强度比在3～8倍之间。为了解释脆性材料压-拉强度比的实验结果，本文对两类不同类型缺陷的压-拉强度比作了分析，得出脆性材料的压-拉强度比可以是大于1.9的任何值。

二、椭球状缺陷的强度分析

设脆性材料中存在着椭球状缺陷，加载后如果椭球很扁的话，将造成上下表面接触。图1给出了这一问题的一个模型。

$$m=\frac{a-b}{a+b}=\frac{1-\delta}{1+\delta}$$

$$\delta=\frac{b}{a}$$

当 $m\to 0$，成为圆孔

当 $m\to 1$，成为裂纹

图1中 A 点处的应力 σ_θ 可以写为[5]：

$$\bar{\sigma}(\alpha,\theta)=\frac{\sigma_\theta}{\sigma}$$

$$=\frac{1-m^2+2m\cos 2\alpha-2\cos 2(\alpha+\theta)-\varepsilon_p(1-3m^2+2m\cos 2\theta)-\varepsilon_q 4m\sin 2\theta}{1+m^2-2m\cos 2\theta} \quad (1)$$

其中：$\varepsilon_p=\frac{p}{\sigma}$

$$\varepsilon_q=\frac{q}{\sigma}$$

$\bar{\sigma}(\alpha,\theta)$是角度 α 和 θ 的函数，下面求 $\bar{\sigma}(\alpha,\theta)$的极值。

由$\frac{\partial\bar{\sigma}}{\partial\alpha}=0$ 得：$\sin 2\theta\cos 2\alpha+(\cos 2\theta-m)\sin 2\alpha=0$ (2a)

由$\frac{\partial\bar{\sigma}}{\partial\theta}=0$ 得：$A+B\cos 2\alpha+C\sin 2\alpha=0$ (2b)

其中：
$$\begin{cases}A=m(1-m^2)(1-2\varepsilon_q)\sin 2\theta-2m\varepsilon_q[2m-(1+m^2)\cos 2\theta]\\ B=-(1-m^2)\sin 2\theta\\ C=2m-(1+m^2)\cos 2\theta\end{cases}$$

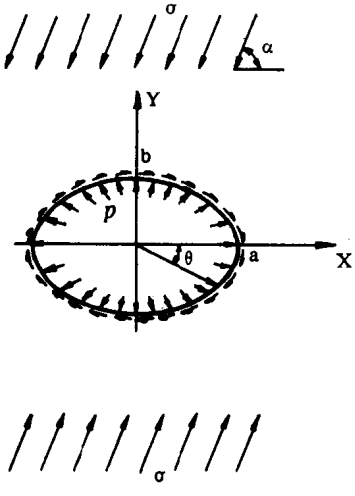

图 1　椭球状缺陷模型

由(2a)得：

$$\cos 2\alpha=\pm\frac{m-\cos 2\theta}{\sqrt{f_m}} \quad (3a)$$

$$\sin 2\alpha=\pm\frac{\sin 2\theta}{\sqrt{f_m}} \quad (3b)$$

将(3)式代入(2b)得：

$$D\pm\sin 2\theta\sqrt{f_m}=0 \quad (4)$$

其中：$D=(1-m^2)(1-2\varepsilon_p)\sin 2\theta-2\varepsilon_q[2m-(1+m^2)\cos 2\theta]$

$f_m=1+m^2-2m\cos 2\theta$

解(4)式即可得到驻点。将(3)式代入(1)得：

$$\bar{\sigma}=\varepsilon_p+\frac{(1-m^2)(1-2\varepsilon_p)\pm 2\sqrt{f_m}-4m\varepsilon_q\sin 2\theta}{f_m} \quad (5)$$

考虑到 α 和 θ 的取值范围：$0°\leqslant\alpha\leqslant 90°$及$-90°\leqslant\theta\leqslant 90°$，那么 $\sin 2\alpha$ 应永远保持正值即 $\sin 2\alpha\geqslant 0$，所以(3)、(4)和(5)式中的正负号这样取：当 $\sin 2\theta>0$，取正号；当 $\sin 2\theta<0$，取负号；当 $\sin 2\theta=0$，正负号均适用。

显然要给出(4)式的解析解是困难的，下面讨论两种情况下(4)式的解。

(一) 缺陷表面不接触

当缺陷的形状比 $\delta=\frac{b}{a}$较大时，在压载下表面不会接触。此时 $\varepsilon_p=\varepsilon_q=0$，则(4)式可写为：

$$(1-m^2)\sin 2\theta\pm\sin 2\theta\sqrt{f_m}=0 \quad (6)$$

1. (6)式的第一个解：

$$\sin 2\theta=0 \qquad (\theta=0\text{ 或 }\theta=90°)$$

$$\cos 2\theta = \pm 1$$

由(3)得：$\sin 2\alpha = 0$，$\cos 2\alpha = \pm 1$（$\alpha = 0$ 或 $\alpha = 90°$）

将上述解代入(5)式得：

$$\bar{\sigma}_1^* = \frac{3-m}{1+m} \quad (\alpha = 0, \theta = \pm 90°) \tag{7a}$$

$$\bar{\sigma}_2^* = \frac{3+m}{1-m} \quad (\alpha = 90°, \theta = 0°) \tag{7b}$$

$$\bar{\sigma}_3^* = \bar{\sigma}_4^* = -1 \quad (\alpha = 0°, \theta = 0°; \alpha = 90°, \theta = \pm 90°) \tag{7c}$$

2. (6)式的第二个解

$$1 - m^2 \pm \sqrt{f_m} = 0$$

因为 $m^2 \leqslant 1$，$f_m \geqslant 0$，所以上式只能取负号。

$$(1-m^2)^2 = 1 + m^2 - 2m\cos 2\theta$$

则：

$$\cos 2\theta = \frac{1+m^2-(1-m^2)^2}{2m}$$

代入(5)式得：

$$\bar{\sigma}_5^* = -\frac{1}{1-m^2} \tag{7d}$$

由(7)式可以看到，当 σ 是拉应力 σ_t 时孔边的最大拉应力 $\sigma'_{\theta\max} = \frac{3+m}{1-m}\sigma_t$；当 σ 是压应力 $-\sigma_c$ 时孔边的最大拉应力是 $\sigma'_{\theta\max} = \frac{1}{1-m^2}\sigma_c$。按最大拉应力破坏准则，当 $\sigma'_{\theta\max} = \sigma_f$ 时可得到单向拉伸强度 σ_t^*

$$\sigma_t^* = \frac{1-m}{3+m}\sigma_f \tag{8a}$$

当 $\sigma'_{\theta\max} = \sigma_f$ 时，可得到单向压缩强度 σ_c^*

$$\sigma_c^* = (1-m^2)\sigma_f \tag{8b}$$

由此可得到压-拉强度比 R

$$R \equiv \frac{\sigma_c^*}{\sigma_t^*} = (1+m)(3+m) \tag{9}$$

由(9)式可以看到：当 $m \to 0$，缺陷为圆孔，$R = 3$；当 $m \to 1$，缺陷为裂纹，$R \to 8$。

（二）缺陷表面接触

当 $\delta = \frac{b}{a}$ 很小时，在压载下缺陷表面可能接触。引入一个摩擦系数 $\eta = \frac{q}{p}$。由于空洞的表面一般比较光滑，所以缺陷的上下表面不会出现啮合咬住，因此必然有 $\eta \leqslant 1$。显然 $p < \sigma$，为计算简单此处仅考虑 $e_y = 0.5$ 的情况。由(4)式得：

$$D_1 \pm \sin 2\theta \sqrt{f_m} = 0 \tag{10}$$

其中：$D_1 = -\eta[2m - (1+m^2)\cos 2\theta]$

将 D_1 代入(10)式，整理后得：

$$2m\cos^3 2\theta - [(1+m^2) + (1+m^2)^2\eta^2]\cos^2 2\theta + 2m[2(1+m^2)\eta^2 - 1]\cos 2\theta + [(1+m^2) - 4m^2\eta^2] = 0 \tag{11}$$

在 $-90° \leqslant \theta \leqslant 90°$ 范围内解上式并将解得的结果代入(5)就可得到在不同摩擦系数 η

和缺陷形状系数 δ 下的压-拉强度比 R。图 2 给出了 R 的变化情况。由(9)式和图 2 可知，对于空洞状缺陷，压-拉强度比 R 在 2～8 之间。

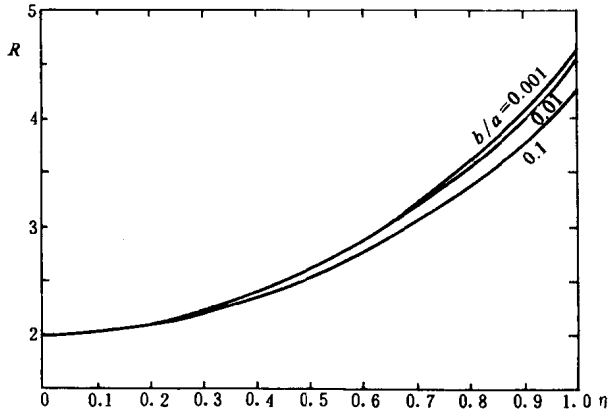

图 2　压-拉强度比 R 的变化

三、片状缺陷的强度分析

设脆性材料中存在着便士形片状裂纹。图 3 给出了这一问题的一个模型。

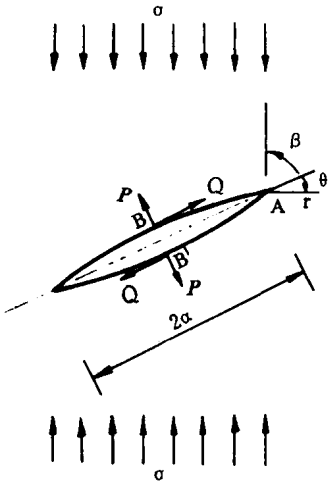

图 3　片状缺陷模型

在外载 σ 的作用下，在裂纹尖端产生应力强度因子 K_{I}^{0} 和 K_{II}^{0}：

$$K_{\mathrm{I}}^{0} = \frac{1}{2}K_0(1-\cos 2\beta) \tag{12a}$$

$$K_{\mathrm{II}}^{0} = \frac{1}{2}K_0 \sin 2\beta \tag{12b}$$

其中：$K_0=\sigma\sqrt{\pi a}$

当 $K_0>0$ 时为拉伸，此时裂纹张开。当 $K_0<0$ 时为压缩，裂纹闭合，因闭合产生的接触载荷 P 和 Q。显然裂纹的闭合是由于 K_{I}^{0} 的存在。又因为 B 和 B' 间的位移与 K_{I}^{0} 成正比，所以假定接触载荷 P 产生的应力强度因子 $K_{\mathrm{I}}^{\mathrm{I}}$ 与 K_{I}^{0} 成正比，即：

$$K_{\mathrm{I}}^{\mathrm{I}} = \varepsilon_{\mathrm{I}} K_{\mathrm{I}}^{0} \tag{13a}$$

裂纹面上的接触载荷 Q 是由于摩擦力的存在而存在的，当然也因为 K_{I}^{0} 的存在而使裂纹面有相互错开的趋势。因此设

$$K_{\mathrm{II}}^{\mathrm{I}} = \varepsilon_{\mathrm{I}} K_{\mathrm{II}}^{0} \tag{13b}$$

由此可得到压载下裂尖 A 点处的应力强度因子：

$$K_{\mathrm{I}} = K_{\mathrm{I}}^{0} - K_{\mathrm{I}}^{\mathrm{I}} = \frac{1}{2}K_0(1-\varepsilon_{\mathrm{I}})(1-\cos 2\beta) \tag{14a}$$

$$K_{\mathrm{II}} = K_{\mathrm{II}}^{0} - K_{\mathrm{II}}^{\mathrm{I}} = \frac{1}{2}K_0(1-\varepsilon_{\mathrm{I}})\sin 2\beta \tag{14b}$$

裂尖的附近场应力为：